IOSR Journal of Applied Physics (IOSR-JAP)
e-ISSN: 2278-4861.Volume 11, Issue 3 Ser. I (May. – June. 2019), PP 18-26
www.iosrjournals.org

Characterization of Silver-Borate Glasses for Biomedical Applications

H. Kamal
Fakeeh College for medical sciences-P.O.Box 2537, Jeddah 21461 KSA
Corresponding Author: H. Kamal

Abstract: *Bioactive glasses were prepared using a progressedmelting cooling technology and are characterized by different spectroscopic techniques. Techniques include X-ray diffraction (XRD), Fourier infrared spectroscopy (FTIR) and UV-VIS.Amorphous nature of prepared glasses was insured using XRD. BO_3 and BO_4structuralgroups' formation upon the addition of silver oxide is measured inside the glass samples using FTIR. Spectral absorption of UV–Visdemonstrated thatthe optical gap increases with increasing Ag_2Oconcentration. The calculated molar volume of the glasswas found to increase Ag_2Oaddition to the glass matrix the calculated value of the molar size because it increases the open structure. There is a good agreement between data obtained from molar volume, infrared spectroscopy, Fourier transform and UV-VIS absorption spectra.*

Keywords: *Silver borate glasses;UV-VIS absorption spectra; Density; Molar Volume; FTIR Spectroscopy and bandgap Energy*

Date of Submission: 18-04-2019 Date of acceptance: 04-05-2019

I. Introduction

B_2O_3 is one of the most general glass formers existing in almost all glasses that are commercial (1-6). Silver doped borate has attracted a great attention because of their good optical properties and high degree of ionic conductivity(3, 5, 7).They are considered to have many applications in the development of solid-state batteries and devices that are involved in electrochemistry. Other species of borate glasses, based on a borate network may be used as a bioactive glass for biomedical applications (6, 8-11).The structure of crystalline and amorphous borate glasses is made up of a random triangleswhich are a network of boroxyl ring units with boron atom is in three-fold coordination (BO_3)(6, 11, 12). In amorphous B_2O_3 glasses, these triangle rings are randomly interconnected and arranged through the loose BO_3 units. The connectivity of the network increases as a result of BO_3units' conversion to four coordinated boron tetrahedral (BO_4) units(6, 11, 13).

Measurement of density is an effective and simple tool to explore any changes that may occur within structure of the glasses(14).Changes in coordination number of geometrical configuration, ions(15), or even in the molar volume of the glass may affect the density. Molar volume is related to the interstitial space within the glass matrix(16).

The main aim of the presented paper is to shed morelights on characterization of silver ion doped borate glasses by different measurementtechniques, UV-VISspectra, FTIR, XRD, density, and molar volume.

II. Sample Preparation

Glass samples of the system [50%B_2O_3 – 10% $CaCO_3$- (20 –x)% Na_2CO_3 – x% Ag_2O where x = 0, 0.25, 0.5 and 1] mole% was attained by weighing the appropriate amounts of chemicals according to the table (1.1).

Table (1.1): A composition of prepared glass samples (by mole).

Sample No.	B_2O_3(mol%)	Ca_2CO_3(mol%)	Na_2CO_3(mol%)	Ag_2O (mol%)
G1	50	24	26	0.0
G2	50	24	25.75	0.25
G3	50	24	25.5	0.5
G4	50	24	25.25	0.75
G5	50	24	25	1

Batches were weighted and melted in crucibles made fromporcelainin an electric furnace at temperatures ranging from 1050˚C - 1250˚C for about 2 hours and rotated at an interval to insure homogeneity. The molten glasses were casted in graphite blocks. After quenching the glass, all the samples were without delay transferred to another annealing furnaceat 400˚C(6, 7, 11, 13).

III. Experimental Techniques

3.1 X ray diffraction (XRD)

X-ray diffraction patterns using a Philips PW1390 X-ray diffractometer equipped with copper Kα radiation of wavelength λ = 1.540 Å using operating voltage 30 kV were used to investigate the internal structural arrangement of atoms or molecules constituting the studied samples examined. All scans were performed in the Bragg's angle (2θ) ranged between 10 and 70°(17).

3.2 UV/vis. optical absorption spectra

In order to study the structural changes results from increasing content of silver oxide to explore their effects on the other optical parameters, a UV/Vis. optical absorption spectrum of each sample was recorded within the wavelength range extended from 200-800 nm. This can be achieved by using a double beam spectrophotometer (Jasco 630 UV/Vis, Japan) using air as a reference sample and with a step of 2 nm. The measurementscan be used to obtain the direct band gap, indirect band gap and Urbach energy values for all prepared glass samples(18).

3.3 FTIR optical absorption spectrum

Fourier transform infrared absorption signals of the studied borate glasses were measured at ambient room temperature in the wavelength range 4000-400 cm^{-1} using a computerized recording FTIR spectrometer (Mattson5000, USA) equipped with mid infrared KBr beam splitter. Powdered samples were mixed with KBr in the ratio 1:100 for quantitative analysis and the weighted mixtures were subjected to a load of $5t/cm^2$ in a revocable i.e to produce clear homogenous discs. Then, the absorption spectra were instantly measured after preparing the discs to avoid moisture attack (13).

3.4 The densityand molar volume

Densitiesof the glass samples were measured by using the suspended-weight method. This method is based on the Archimedes principle. Xylenewith a density (0.871 g/cm^3 at 25°C) isused as the immersion liquid. The samples were weighed on a balance enclosed in a constant temperature box; the temperature is controlled at 22°C for all samples, with an accuracy of ± 0.1°C.

All the measurements were made using a digital balance (M/S Sartorius, model BP 221S, USA). Thedensity of a glass was taken as the average of at least four samplesto get an accurate value of density. The experimental error in the density was estimated to be ± 0.01 g/cm^3. The samples were suspended by a fine nickel-chrome wire diameter 0.1 mm.

The density was calculated according to the formula.

$$d = \frac{W_a}{(W_a - W_b)xD} \ldots\ldots\ldots\ldots\ldots\ldots\ldots\ldots(1.1)$$

WhereW_a is the weight of the sample in air, W_b is the weight of the sample in xylene and D is the density of buoyancy at room temperature.

Corrections were done for the submerged and unsubmerjedparts of the suspended wire in xylene and air respectively as well as for the force due to surface tension. Fourwell-tempered, bubble-free glass samples from different batches of the same composition were measured individually and the average values of their densities taken.

The molar volume of all glass samples can be calculated by using the molecular weight of the glasses. The molar volume values were calculated by using the obtained densities and weight of one mole of the sample, with the help of the following equation:

$$V_m = \sum_i \frac{M_i}{d} \ldots\ldots\ldots\ldots\ldots\ldots\ldots\ldots (1.2)$$

Miis the molar mass of the glass and Mi = C_iA_i. Here Ci and Ai are the molar concentrations and molecular weights of the ith component, respectively and d is measured density (16).

3.5. pH measurements

Changes in solution pH wereanalyzed when bioactive glassesare dissolved in simulated body fluids (SBF). pH values were measured by a pH- meter (Jenway-3150 Premier Portable pH/mV/ Temperature Meter with an accuracy of 0.01).The calibration of the electrode against buffer solution was performed at an interval of 48 h (19).

IV. Results and Discussion

From the different types of measurements mentioned discussed above, the results obtained can be discussed as follows:

4.1 X-Ray Diffraction Analysis

X-ray diffraction (XRD) is one of the most analytical non-destructive techniques that give information related to the microstructure, physical characteristics and chemical composition of studied glasses(20).

The X-ray powder analysis of samples (Fig. 1.1) reveals the presence of two broad humps and doesn't exhibit any detectable peaks. This confirms the correct preparation procedures of glass samples.

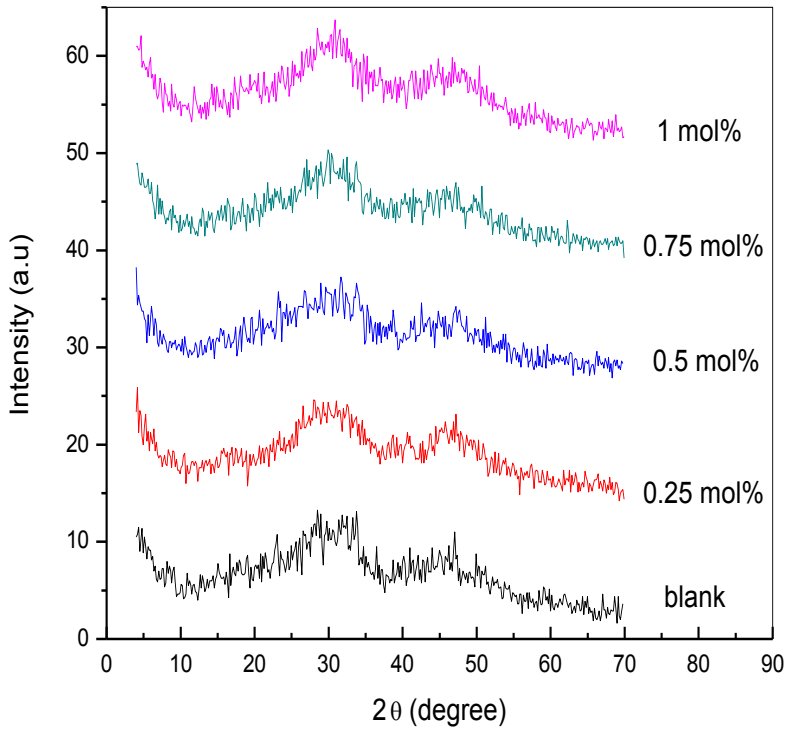

Figure (1.1): XRD of the glass samples with different contents of Ag_2O.

4.2 Density and Molar Volume

The density measurement is considered to be greatlyimportant tool to distinguish the structural changes of the glass network(21). There is a relation between the structure of the glass and density is since, the density is believed to change obviously(22). The density depends on the coordination number, non-bridging oxygen's and existence of the cross-linking in structural units(23). Basically,parameters mentioned above influence the packing of the structural units and finally change the volume of the bulk glass samples. Since, the network structures and arrangement of building units can used to describe the molar volume of glassesas it deals directly with the spatial structure of the oxygen network(4).

The measured density and calculated molar volumeof the glass samples are shown in Table (2.2). The density of present samples appears to increasegradually from 2.467 to2.442gm/cm^3 with increases of Ag_2O content. This may be attributed to mightbe the formation on non-bridging oxygen (NBOs). The behavior of molar volume essentially depends on the density of glasses and as expected in the present glasses case, it follows a trend opposite to density.

The variation of density and molar volume with concentration of Ag_2O is shownin figure (1.2)

From the calculated molar volume, it can be seen that there is an increase in molar volume with increasing content of Ag_2O. This increase could be attributed to Ag_2O opening the glass network. This increase may also reveal the network homogeneity thus, reflects the strengthening of internal chemical bonds.

Table (1.2): Density (ρ), molar volume (Vm) of borate glasses doped with Ag_2O

Sample	Ag_2O content (mol%)	Density (gm cm^{-3}) ± 0.002	Molar volume (cm^3)
G1	0	2.467	28.489
G2	0.25	2.462	29.496
G3	0.5	2.459	30.532
G4	0.75	2.451	31.502
G5	1	2.442	32.498

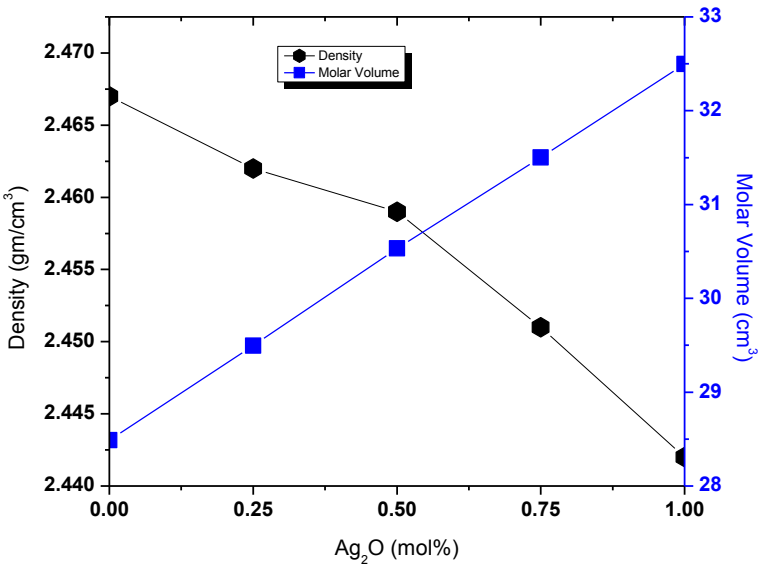

Figure (1.2): Compositional dependence of density (ρ), and molar volume (V_m) for borate glass doped Ag_2O

4.3 Solubility Measurement

It is well known thatthe main processes by which silicate, borosilicate and borate bioactive glass degrade and convert to an HA-like material have attracted many investigator (24-26). The degradation kinetics of the glass and the conversion to hydroxyapatite have been evaluatedin vitro by immersing the glass into aqueous phosphate solution at normal human body temperature at 37 °C, and measuring the weight loss percentagefor glass as a function of immersion time (11).

Fig (1.3) shows the changes occur in pH upon submergingglass samples into phosphate solution. pH changes were recorded at different time intervals up to 30 days. pHstarts (8.05~8.3) and reaches a maximum valuesdepending on the concentration of silver oxide percentage added to the glass matrix. The increase in pH occurs when all glasses are soaked into solution within the first 5 days of immersion. The degradation is also be associated with dissolution of ions and soluble some soluble species (e.g. Na^+ and $(BO_3)^{3-}$, depending depends mainly on the glass composition) into the solution and leaching of cations out of the glass. Besides that,sodium ions exchange with H^+ ions insolution. In addition, these conversion products has been characterized using different structural, chemical and micro chemical techniques(27).

The concentration of Ag_2O strongly influences the acid or base properties on surface of bioactive glass. Also, the amount of Ca plays an important role in interaction of glass and phosphate solution(28). Molar adsorption heats developed by the interaction of phosphate solution and glasses indicate the possibility of cooperative effects among calcium cations, which are present in relatively high amounts(29).

It is well known that addition of sodium to borate glasses increases the chemical durability since it decreases the weight loss(24). Figure (1.4) shows the percent weight loss of all prepared glass samples during different immersion periods. The prepared glasses possesses a considerable range of degradability greater than that in case of silicates, this is because the prepared samples experience a weight loss approximately 14% in about 30 days of immersion into phosphate solution. All results in weight loss measurements agree well with that obtained of other well-accepted soluble bioactive glass compositions (6, 7, 11, 13).

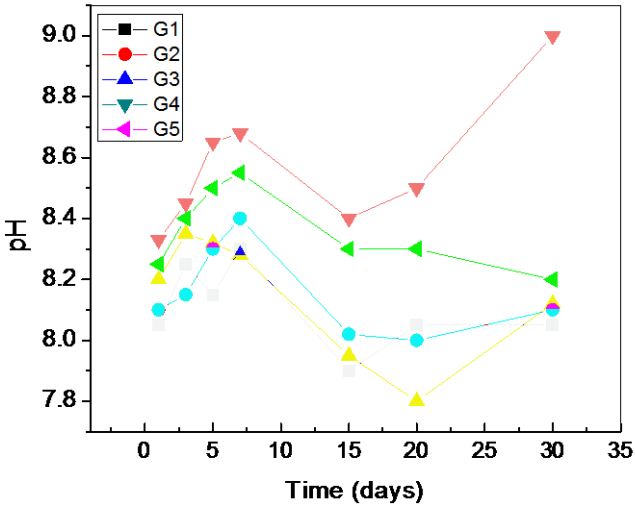

Figure (1.3): pH dependence of borate glass doped Ag_2O.

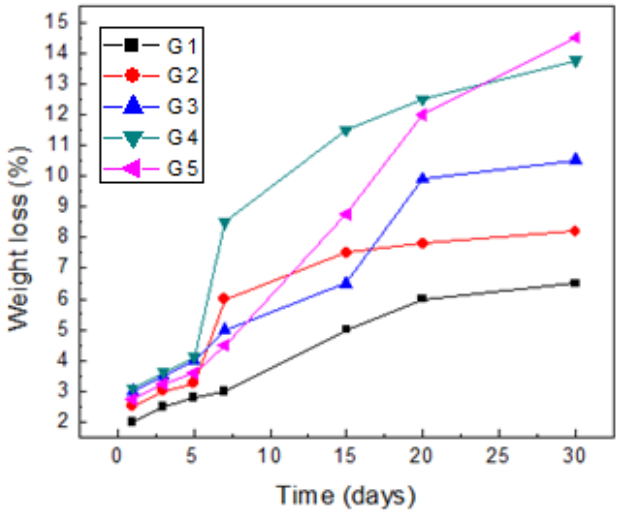

Figure (1.4): Weight loss dependence of borate glass doped Ag_2O.

4.3 FTIR Analysis

FT-IR spectroscopic analysis is mainly considered as a powerful tool for analysis of materials composed or contains different functional groups including organic, inorganic and mixed samples that include polymers and glasses(30). It is a simple and efficient technique that carriesa large amount of structural information(31). So, it has been used here to get this get more structural information. Vibrational spectroscopy analysis (IR) used to import information related to the structural and chemical composition.

Figure (1.5) represents FTIR spectroscopy of prepared borate bioactive glasses. The figure indicates that samples have mainly specific vibrational modes. These modes are attributed to B-O bond stretching of the tetrahedral BO_4 units, bending of B-O-B linkages in the borate networks, asymmetric stretching relaxation of the B-O bond of trigonal BO_3 units(6, 7, 10, 11, 13). These vibrational modes were observed at 700cm^{-1}, between the wavenumber range1600~1200cm^{-1} andbetweenwavenumber range1200~800cm^{-1}respectively.Stretching of the BO_4 structural appears around 1050 cm^{-1}. Bending vibrations of BO_3 triangles and stretching vibrations of BO_3 units with non-bridging oxygen appeared at the band in the range 665 ~ 695 cm^{-1}(6, 7, 10, 11, 13). Bands centered at 1630 cm^{-1} and 2330 cm^{-1} are attributed to O-H bending due to absorption in this region and the existence of some adsorbed water. The band 535~550 cm^{-1} may be due to vibrations of sodium cations through the glass network. The band around 1450 cm^{-1} can be assigned to B-O stretching vibrations and is mainly the linkage between oxygen and different groups as well as B-O bridging between boroxol rings and trigonal BO_3(6, 7, 10, 11, 13).

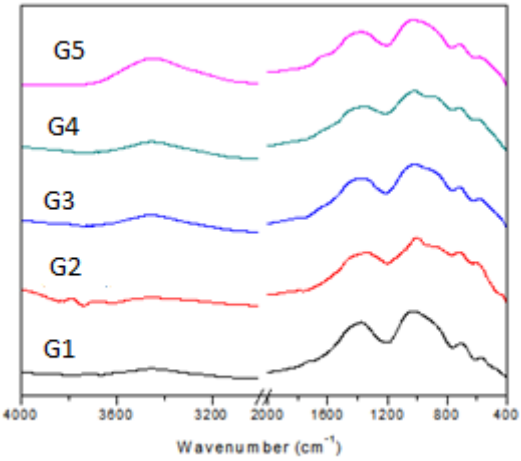

Figure (1.5): FTIR of the glass samples with different contents of Ag_2O.

4.4 Determination of optical energy gap (Eg).

It is well-known that studying optical absorption spectral data suggests useful information about band structure of different compounds(32). During the absorption process, an electron move from a lower to higher energy state through absorption of a specified energy in the form of photons(33). Different types of possible electron transitions can be established by the changes in the absorbed radiation.

Evaluation of optical band gap ($E_g = hc/\lambda$) occurs by noticing the sudden change in the fundamental absorption. This sudden change can be defined as (absorption edge)

Absorption coefficient (α) represent the relative rate of decrease in light intensity given by;

$$\boldsymbol{\alpha = 2.303\frac{A}{d}} \qquad (\mathbf{2-2})$$

Where(A) is the absorbance and (d) is the sample thickness.

The relation between the absorption coefficient of amorphous materials and energy of the incident photon can be presented as follows.

$$(\boldsymbol{\alpha h\nu}) = \boldsymbol{C(h\nu - E_g)^n for h\nu > E_g} \qquad (\mathbf{2-3})$$

$$(\boldsymbol{\alpha h\nu}) = \boldsymbol{0 for h\nu < E_g} \qquad (\mathbf{2-4})$$

where E_g is the optical energy gap, C is a constant and n is the power that can take values 1, 2, 3, 1/2 and 3/2, this depends on the nature of the electron transitions responsible for the optical absorption (1/2 for direct electronic transition in the k space and 2 for indirect electronic transition across indirect energy gap and 1, 3 for forbidden transitions).

Optical band gaps were calculated using absorption spectra for direct and indirect transitions for all prepared glass samples. The absorption coefficient α(ν) is related to the optical band gap energy (Eg) at the higher photon energy or in the Tauc region. Then, according to Davis and Mott (34),

$$\boldsymbol{\alpha}(\nu) = \frac{\boldsymbol{B(h\nu - E_g)^n}}{\boldsymbol{h\nu}} \ldots\ldots\ldots\ldots\ldots\ldots (\mathbf{1})$$

Where n is the index that depends on the nature of electronic inter-band transitions. It has different values according to the type of transition; direct or indirect. So that, n= ½ for allowed direct transitions, 3/2 for forbidden direct transitions, 2 for indirect allowed transitions, 3 for indirect forbidden transitions. B is a constant, E_g is the optical band gap energy, hν is the energy of the incident photon.

Extrapolation of the linear portion of the plots between $(\alpha h\nu)^{1/2}$ and hν to the X-axis where $(\alpha h\nu)^{1/2}=0$ gives the values of the band gap energy.

α(ν) is an exponential function of photon energy (hν) at the lower photon energy or in the Urbach region as derived by the Urbach,

$$\boldsymbol{\alpha}(\nu) = \boldsymbol{\alpha_o exp\frac{h\nu}{E_u}} \ldots\ldots\ldots\ldots\ldots\ldots\ldots (\mathbf{2})$$

where $\boldsymbol{\alpha_o}$ is a constant, Eu is the Urbach energy which indicates the band tailingwhich is the width of the localized states in the normally forbidden band gap(35). Eu is related to the optical electronic transition between a localized band tail and extended band. Urbach energy values (ΔE) were calculated by taking the reciprocals of the slopes of the linear portion in the lower photon energy region of these curves.The Urbach energy is found out from the graph is listed in Table (1.3).

The indirect and direct transitions can be determined by plotting a function of photon energy (E=hυ)

and $(\alpha h\upsilon)^2$ and optical band gaps for can be calculated respectively. The respective values of E_{opt}were obtained by extrapolating to $(\alpha h\nu)^{1/2} = 0$ for indirect transitions and $(\alpha h\nu)^2 = 0$ for direct transitions(35).

Figures (1.5, 1.6) show plots for the direct band gap, indirect band gap and Urbach energies for the present samples and their values are listed in Table (2.2).From the results, it can be shown that E_{opt}increases with increasing Ag_2O content. This may results in some change in bonds which is reflected by lowering of band gap values. The noticed change may also arise from the photon-lattice interaction (4, 6, 7, 13). The shift of the absorption band to the higher energy corresponds to the increase in NBO's making the structure open. These results agree with our results for molar volume which also show an increase confirming the opening of a structure.

The behavior of the optical transition is similar to the trend of the density data. The increase in band gap value may be related to compactness of the glass structure. Moreover, the increasing values in band gaps due to the formation of BO_4 units or the formation of bridging oxygen (4, 6, 7, 13).

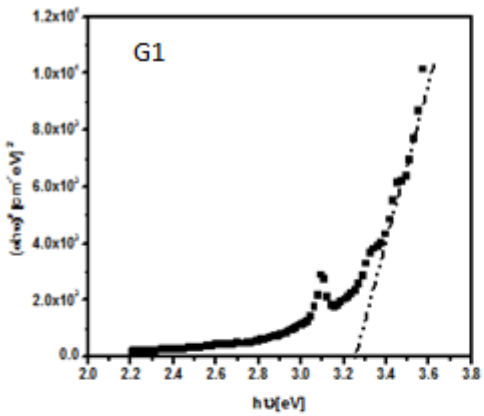

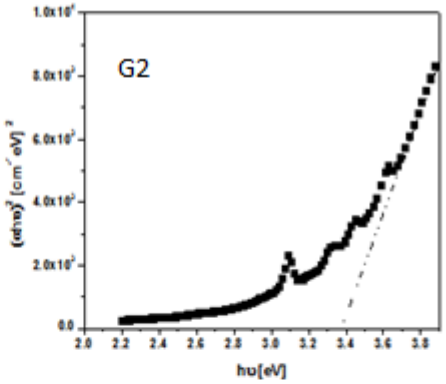

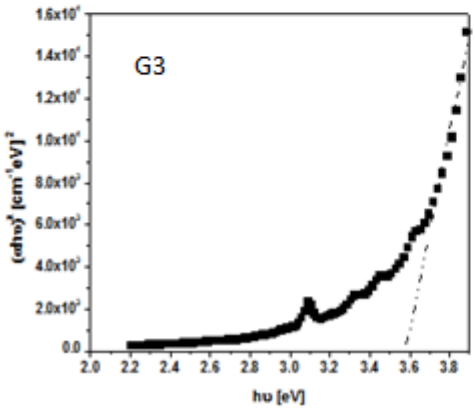

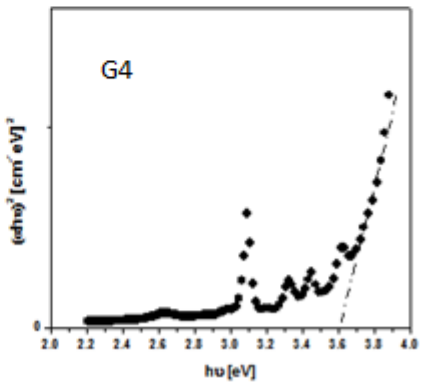

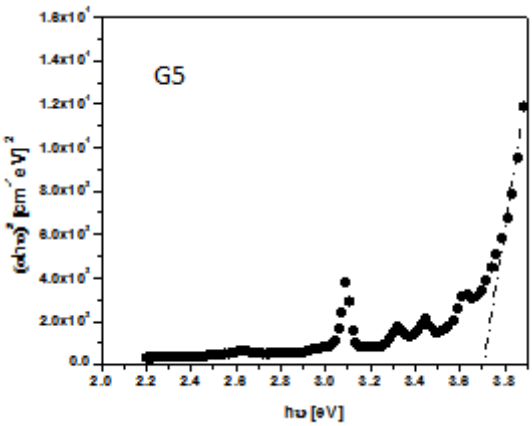

Figure (3.5): Direct optical band gap as a function of photon energy for borate glasses doped with Ag_2O.

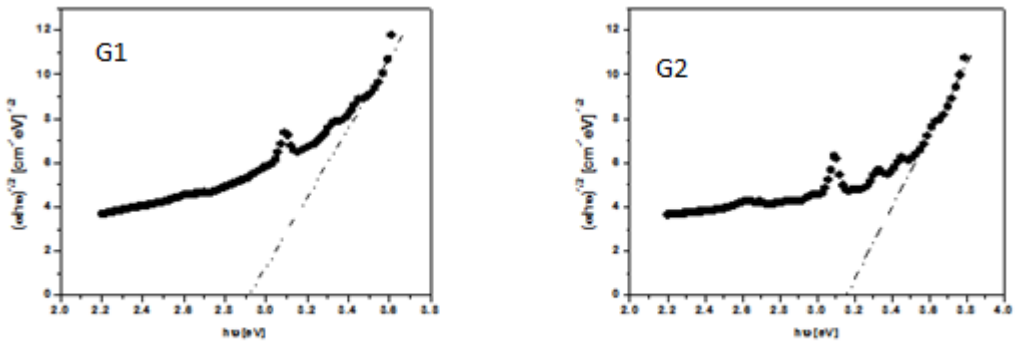

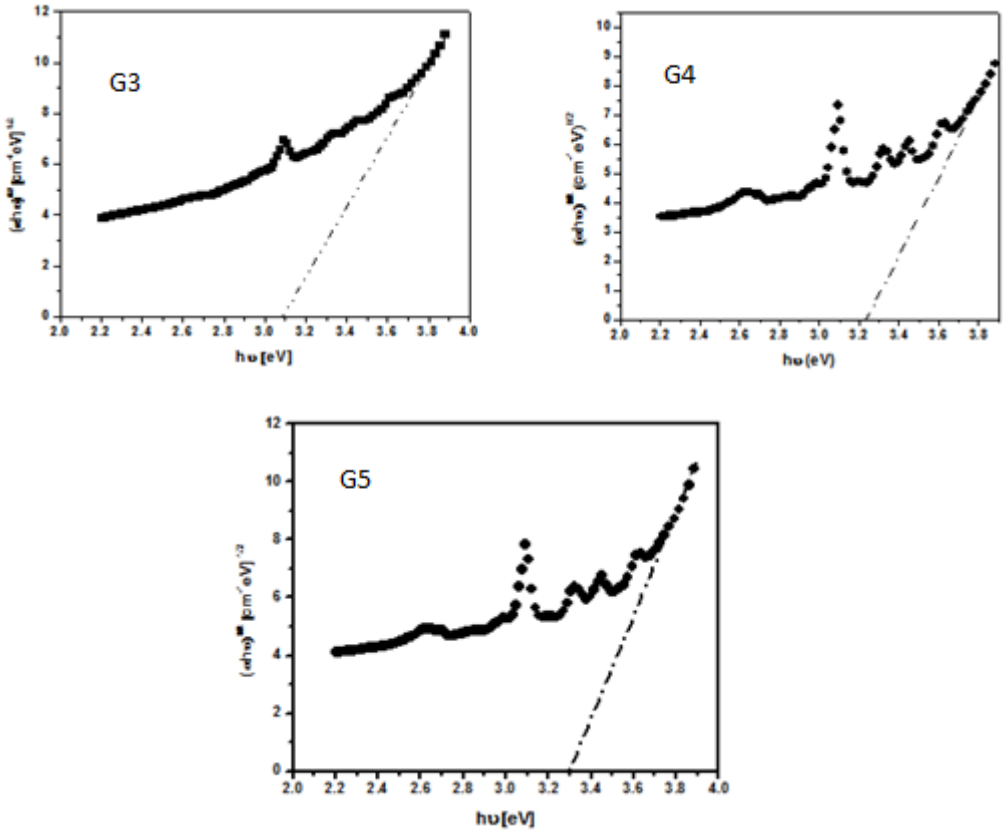

Figure (3.6): Indirect optical band gap as a function of photon energy for borate glasses doped with Ag_2O.

Table (1.3): ***Direct and*** indirect optical band gap as a function of photon energy for borate glasses doped with Ag_2O.

Sample No.	G_1	G_2	G_3	G_4	G_5
Direct band gap (eV)	3.28	3.39	3.58	6.62	3.71
Indirect band gap (eV)	2.94	3.09	3.15	3.25	3.3
Urbach energy (eV)	0.55	0.61	0.72	0.79	0.86

V. Conclusion

XRD results reveal that the prepared glasses were amorphous. Ultraviolet-Visible (UV-VIS) absorption spectra indicated that the optical band gap increases with the increase of Ag_2O content. Urbach energy is observed between 0.55 - 0.86eV. The measured pH values and percentage of weight lossfor glass have increased with the Ag_2O addition.Density and molar volumes of the prepared samples increase gradually with the increase of Ag_2O content due to closing of the structure of glasses. FTIR results reveal that groups of BO_3 and BO_4work as network structural groups while sodium and silver appear in interstitial positions.

References

[1]. Ardelean I, Cora S, Ioncu V. Structural investigation of $CuO-Bi_2O_3-B_2O_3$ glasses by FT-IR, Raman and UV-VIS spectroscopies. Journal of optoelectronics and advanced materials. 2006;8(5):1843-7.

[2]. Gressler CA, Shelby JE. Properties and structure of PbO- PbF_2- B_2O_3 glasses. Journal of Applied Physics. 1989;66(3):1127-31.

[3]. Paul A. Chemistry of glasses: Springer Science & Business Media; 1989.

[4]. Shelby JE. Introduction to glass science and technology: Royal Society of Chemistry; 2007.

[5]. Varshneya AK. Fundamentals of inorganic glasses: Elsevier; 2013.

[6]. Kamal H, Hezma A. Structure and Physical Properties of Borosilicate as Potential Bioactive Glasses. Silicon. 2017:1-8.

[7]. Kamal H. Structure and physical properties of silver borate bioactive glasses. Res J Pharmaceut Biol Chem Sci. 2014;5(5):832.

[8]. Bengisu M. Borate glasses for scientific and industrial applications: a review. Journal of materials science. 2016;51(5):2199-242.

[9]. Lev O, Wu Z, Bharathi S, Glezer V, Modestov A, Gun J, et al. Sol− gel materials in electrochemistry. Chemistry of Materials. 1997;9(11):2354-75.

[10]. Rahaman MN, Day DE, Bal BS, Fu Q, Jung SB, Bonewald LF, et al. Bioactive glass in tissue engineering. Acta biomaterialia. 2011;7(6):2355-73.

[11]. Abdelghany A, Kamal H. Spectroscopic investigation of synergetic bioactivity behavior of some ternary borate glasses containing fluoride anions. Ceramics international. 2014;40(6):8003-11.

[12]. Saritha D, Markandeya Y, Salagram M, Vithal M, Singh A, Bhikshamaiah G. Effect of Bi2O3 on physical, optical and structural studies of $ZnO–Bi_2O_3–B_2O_3$ glasses. Journal of Non-Crystalline Solids. 2008;354(52-54):5573-9.

[13]. Kamal H, Abdelghany A. Effect of Transition Metal Addition in the Bioactivity of Borate Bioglass Dental Materials.

[14]. Bajaj A, Khanna A, Chen B, Longstaffe JG, Zwanziger U-W, Zwanziger J, et al. Structural investigation of bismuth borate glasses and crystalline phases. Journal of Non-Crystalline Solids. 2009;355(1):45-53.

[15]. Korecz L, Saghier A, Burger K, Tzschach A, Jurkschat K. Determination of the coordination number and geometry of the coordination sphere of the central tin atom in stannatrane complexes by Mössbauer spectroscopy. Inorganica Chimica Acta. 1982;58:243-9.

[16]. Singh N, Singh KJ, Singh K, Singh H. Comparative study of leManusciptyad borate and bismuth lead borate glass systems as gamma-radiation shielding materials. Nuclear Instruments and Methods in Physics Research Section B: Beam Interactions with Materials and Atoms. 2004;225(3):305-9.

[17]. ElBatal H, Azooz M, Khalil E, Monem AS, Hamdy Y. Characterization of some bioglass–ceramics. Materials Chemistry and Physics. 2003;80(3):599-609.

[18]. Kumar G, Thomas J, George N, Kumar B, Radhakrishnan P, Nampoori V, et al. Optical absorption studies of free (H2Pc) and rare earth (RePc) phthalocyanine doped borate glasses. Physics and chemistry of glasses. 2000;41(2):89-93.

[19]. Huang W, Day DE, Kittiratanapiboon K, Rahaman MN. Kinetics and mechanisms of the conversion of silicate (45S5), borate, and borosilicate glasses to hydroxyapatite in dilute phosphate solutions. Journal of Materials Science: Materials in Medicine. 2006;17(7):583-96.

[20]. Azároff LV, Kaplow R, Kato N, Weiss RJ, Wilson A, Young R. X-ray Diffraction: McGraw-Hill New York; 1974.

[21]. Guthrie M, Tulk C, Benmore C, Xu J, Yarger J, Klug D, et al. Formation and structure of a dense octahedral glass. Physical Review Letters. 2004;93(11):115502.

[22]. Krogh-Moe J. The structure of vitreous and liquid boron oxide. Journal of Non-Crystalline Solids. 1969;1(4):269-84.

[23]. Brow RK. the structure of simple phosphate glasses. Journal of Non-Crystalline Solids. 2000;263:1-28.

[24]. Fu Q, Rahaman MN, Fu H, Liu X. Silicate, borosilicate, and borate bioactive glass scaffolds with controllable degradation rate for bone tissue engineering applications. I. Preparation and in vitro degradation. Journal of Biomedical Materials Research Part A. 2010;95(1):164-71.

[25]. Rahaman MN, Day DE, Sonny Bal B, Fu Q, Jung SB, Bonewald LF, et al. Bioactive glass in tissue engineering. Acta biomaterialia. 2011;7(6):2355-73.

[26]. Gao C, Gao Q, Bao X, Li Y, Teramoto A, Abe K. Preparation and in vitro bioactivity of novel mesoporous borosilicate bioactive glass nanofibers. Journal of the American Ceramic Society. 2011;94(9):2841-5.

[27]. Thind K, Singh K, Kumar V, Sharma G, Singh D, Singh D. Compositional dependence of in-vitro bioactivity in sodium calcium borate glasses. Journal of Physics and Chemistry of Solids. 2009;70(8):1137-41.

[28]. Liu X, Pan H, Fu H, Fu Q, Rahaman MN, Huang W. Conversion of borate-based glass scaffold to hydroxyapatite in a dilute phosphate solution. Biomedical Materials. 2010;5(1):015005.

[29]. Abdelghany A. Novel method for early investigation of bioactivity in different borate bio-glasses. Spectrochimica Acta Part A: Molecular and Biomolecular Spectroscopy. 2013;100:120-6.

[30]. Mansur HS, Sadahira CM, Souza AN, Mansur AA. FTIR spectroscopy characterization of poly (vinyl alcohol) hydrogel with different hydrolysis degree and chemically crosslinked with glutaraldehyde. Materials Science and Engineering: C. 2008;28(4):539-48.

[31]. Efimov A. Quantitative IR spectroscopy: applications to studying glass structure and properties. Journal of Non-Crystalline Solids. 1996;203:1-11.

[32]. Ebraheem S, El-Saied A. Band gap determination from diffuse reflectance measurements of irradiated lead borate glass system doped with TiO2 by using diffuse reflectance technique. Materials Sciences and Applications. 2013;4(05):324.

[33]. Margha FH, Abdelghany AM. Bone bonding ability of some borate bio-glasses and their corresponding glass-ceramic derivatives. Process Appl Ceram. 2012;6(4):183-92.

[34]. Davis E, Mott N. Conduction in non-crystalline systems V. Conductivity, optical absorption and photoconductivity in amorphous semiconductors. Philosophical Magazine. 1970;22(179):0903-22.

[35]. Mahr H. Absorption band shape and Urbach's rule of localized excitons. Physical Review. 1963;132(5):1880.